Fifty-Fifth Annual Allerton Conference
Allerton House, UIUC, Illinois, USA
October 3-6, 2017

Network-cognizant Model Reduction of Grid-tied Three-phase Inverters

Victor Purba, Sairaj V. Dhople
University of Minnesota
E-mails: {purba002, sdhople}@umn.edu

Saber Jafarpour, Francesco Bullo
University of California at Santa Barbara
E-mails: {saber.jafarpour, bullo}@engineering.ucsb.edu

Brian B. Johnson
National Renewable Energy Laboratory
E-mail: brian.johnson@nrel.gov

***Abstract*—Power-electronics inverters are expected to satisfy a significant fraction of system load in next-generation power networks with the growing integration of renewable resources and flexible loads. Typical dynamical models for grid-tied inverters are nonlinear and composed of a large number of states; therefore it is impractical to study systems with many inverters when their full dynamics are retained. In our previous work, we have shown that a system of parallel-connected grid-tied three-phase inverters can be modeled as one aggregated inverter unit with the same structure and state-space dimension as any individual inverter in the system. Here, we extend this result to networks with arbitrary topologies by leveraging a classical aggregation method for coherent synchronous generators in transmission networks, and a linear approximation of the AC power-flow equations to ease computational burden. Numerical simulation results for a prototypical distribution feeder demonstrate the accuracy and computational benefits of the approach.**

I. Introduction

Power electronics inverters are being integrated in large numbers in distribution networks with rapid deployment of renewable resources, energy storage, and flexible loads. Indeed, while it is obvious that DC resources, such as photovoltaic panels, fuel-cells, and batteries, need inverters to supply AC power to the grid, inverters are also used as grid interfaces for wind turbines with variable frequency output. Since such distributed energy resources will serve a majority of loads in the next-generation power network, it is critical to develop scalable and accurate modeling tools to study the dynamic behavior of systems with large numbers of inverters. To this end, this work primarily focuses on reducing the model complexity of multi-inverter systems. We study a grid-following three-phase voltage source inverter with an output LCL filter, current controller, power controller, and phase-locked loop (PLL). Without loss of generality, we focus on the 15-state model developed in [1]–[4]. (Indeed, this model order demonstrates the analytical inconvenience and computational burden involved in examining large collections of networked grid-tied inverters.)

We build on our preliminary work [5], where we proposed a lumped-parameter reduced-order model for three-phase grid-tied inverters that are connected in parallel to a common bus. In particular, we derived an aggregate reduced-order model that captures the dynamical behavior of the multi-inverter system while presenting the modeling complexity and structure of an individual inverter in the parallel collection. In this work, we extend the analysis to examine networks of identical three-phase grid-tied inverters that are connected within an arbitrary electrical network fed by an infinite bus (modeling the rest of the network). The approach we outline leverages an aggregation method previously used for synchronous generators [6]–[8], where coherent generators are transferred to an auxiliary bus. Ideal transformers connect this auxiliary bus to the original buses and this preserves the power flows in the network. Subsequently, the generators are replaced by an equivalent aggregate generator model. While the notion of coherency does not perfectly translate to the distributed generation setting in general [9], [10], this approach is useful since it allows us to leverage our previous result to aggregate inverters once they are all connected to one (i.e., the auxiliary) bus. To determine the turns ratios of the transformers, one needs the voltages at the point of interconnection of the inverters which are governed by the nonlinear AC power flow equations. To circumvent the computational burden of solving a nonlinear AC power flow to perform the model reduction, we resort to linear approximations in Cartesian coordinates that have been extensively studied in the literature and received increased attention recently [11]–[13]. In particular, the inverter terminal voltages are obtained by solving for perturbations in Cartesian coordinates around a nominal voltage profile from the set of original power-flow equations while neglecting quadratic terms.

Arguably, one of the most common model-reduction methods for inverter-based systems has been singular perturbation [14]. For instance, the approaches in [15]–[17] all apply singular perturbation to examine islanded inverter-based microgrids. Also related to this effort is the aggregate model developed in [18] for islanded inverters. In contrast, our proposed model reduction method focuses on a collection of grid-tied three-phase inverters with conventional grid-following current controllers and PLLs. Possible applications of this reduced-order model are in the study of low-inertia systems [19]–[21] and large-scale system modeling [22].

This work was supported by the U.S. Department of Energy (DOE) Solar Energy Technologies Office under Contract No. DE-EE0000-1583.

The remainder of this paper is organized as follows. In Section II, we introduce the three-phase grid-connected inverter model. We revisit—albeit summarily—the reduced-order model derivation for the parallel interconnection in Section II, and outline the network-cognizant approach in Section III. To validate the proposed methods, we compare numerical simulations for an illustrative network to its corresponding reduced-order system in Section IV. Finally, concluding remarks and directions for future work are given in Section V.

Notation: The matrix transpose is denoted by $(\cdot)^{\mathrm{T}}$. The spaces of $N \times 1$ real- and complex-valued vectors are denoted by $\mathbb{R}^N$ and $\mathbb{C}^N$, respectively; and $\mathbb{R}^{N\times N}$ and $\mathbb{C}^{N\times N}$ denote the spaces of $N \times N$ real- and complex-valued matrices, respectively. A diagonal matrix formed with the entries of vector x is denoted by $\mathrm{diag}(x)$; 1_n and 0_n denote n-dimension vectors of all one and all zero entries, respectively; $0_{m\times n}$ denotes an m-by-n matrix of all zeros. Furthermore, $j = \sqrt{-1}$; the magnitude, angle, real and imaginary components of a complex variable x are denoted by $|x|$, $\angle x$, $\mathrm{Re}\{x\}$, and $\mathrm{Im}\{x\}$, respectively, and the matrix conjugate transpose is denoted by $(\cdot)^{\mathrm{H}}$. The cardinality of set $\mathcal{A}$ is denoted by $|\mathcal{A}|$.

II. The Inverter Model and Aggregation of Parallel-connected Inverters

We begin this section with some preliminaries that cover the model of a single inverter and then overview the aggregation approach for N parallel-connected inverters.

A. Inverter Model

We place the following discussion in context of the inverter model sketched in Fig. 1a.

1) Reference-frame transformations: Three-phase signals $(x^{\mathrm{a}}, x^{\mathrm{b}}, x^{\mathrm{c}})$ are transformed to equivalent DC signals $(x^{\mathrm{d}}, x^{\mathrm{q}})$ using Park's transformation:

$$\begin{bmatrix} x^{\mathrm{d}} \\ x^{\mathrm{q}} \end{bmatrix} = \frac{2}{3}\begin{bmatrix} \cos(\delta) & \cos(\delta - \frac{2\pi}{3}) & \cos(\delta + \frac{2\pi}{3}) \\ -\sin(\delta) & -\sin(\delta - \frac{2\pi}{3}) & -\sin(\delta + \frac{2\pi}{3}) \end{bmatrix}\begin{bmatrix} x^{\mathrm{a}} \\ x^{\mathrm{b}} \\ x^{\mathrm{c}} \end{bmatrix} =: \frac{2}{3}\Psi(\delta)\begin{bmatrix} x^{\mathrm{a}} \\ x^{\mathrm{b}} \\ x^{\mathrm{c}} \end{bmatrix}, \tag{1}$$

where δ is the instantaneous angle from the PLL. The abc-dq block in Fig. 1a signifies the transformation.

In a system of inverters, the controller for each inverter runs its own dq reference frame. For analytical convenience, inverter outputs and network variables should be represented in a common reference frame. To do so, we also introduce a global DQ frame with phase denoted by δ_g, frequency ω_g, and transformation matrix $\Psi(\delta_g)$. The transformation of variables between local and global reference frames is captured by:

$$\begin{bmatrix} x^{\mathrm{D}} \\ x^{\mathrm{Q}} \end{bmatrix} = \begin{bmatrix} \cos(\delta_g - \delta) & -\sin(\delta_g - \delta) \\ \sin(\delta_g - \delta) & \cos(\delta_g - \delta) \end{bmatrix}\begin{bmatrix} x^{\mathrm{d}} \\ x^{\mathrm{q}} \end{bmatrix}. \tag{2}$$

2) State-space Model for the Inverter Dynamics: A block diagram of the inverter control architecture is illustrated in Figure 1a. We assume a voltage source inverter (VSI) with a full bridge topology and an output LCL filter (L_f, C_f, L_c). The control architecture consists of an inner-loop current controller, an outer-loop power controller, and a phase-locked loop (PLL). We briefly overview the individual controllers next.

The power controller consists of two low pass filters (with cut-off frequency ω_c) and two PI controllers (with PI gains $k_P^p, k_Q^p, k_P^i, k_Q^i$). The reference inputs to the controller are the active- and reactive-power setpoints (denoted by p^* and q^*, respectively), its outputs are the references for the current controller. The current controller consists of two PI controllers (with PI gains $k_{i\mathrm{d}}^p, k_{i\mathrm{q}}^p, k_{i\mathrm{d}}^i, k_{i\mathrm{q}}^i$) and feedforward terms, with outputs to be the reference for the terminal voltage v_i. For an ideal inverter we have v_i to be the same as its reference (see Fig. 1a). The PLL consists of a low pass filter (with cut-off frequency $\omega_{c,\mathrm{PLL}}$) and a PI controller (with PI gains k_{PLL}^p and k_{PLL}^i). It synchronizes with the grid by modulating the angle δ such that v_g^{d} diminishes to 0 asymptotically.

The dynamics of the controller and filter can be compactly expressed in state-space form as follows [5]:

$$\dot{x} = Ax + Bu_1 + g(x, u_2), \tag{3}$$

with states

$$x = [i_l^{\mathrm{d}}, i_l^{\mathrm{q}}, i_o^{\mathrm{d}}, i_o^{\mathrm{q}}, v_o^{\mathrm{d}}, v_o^{\mathrm{q}}, \gamma^{\mathrm{d}}, \gamma^{\mathrm{q}}, p_{\mathrm{avg}}, q_{\mathrm{avg}}, \phi_p, \phi_q, v_{\mathrm{PLL}}, \phi_{\mathrm{PPL}}, \delta]^{\mathrm{T}},$$

and inputs:

$$u_1 = [p^*, q^*]^{\mathrm{T}}, \quad u_2 = [v_g^{\mathrm{a}}, v_g^{\mathrm{b}}, v_g^{\mathrm{c}}]^{\mathrm{T}} = v_g^{\mathrm{abc}}.$$

In order to show the entries of matrices $A \in \mathbb{R}^{15\times 15}$, $B \in \mathbb{R}^{15\times 2}$, and function $g : \mathbb{R}^{15} \times \mathbb{R}^3 \rightarrow \mathbb{R}^{15}$, we partition the state vector as $x = [x_{LCL}^{\mathrm{T}}, x_{\mathrm{CC}}^{\mathrm{T}}, x_{\mathrm{PC}}^{\mathrm{T}}, x_{\mathrm{PLL}}^{\mathrm{T}}]^{\mathrm{T}}$, where $x_{LCL} = [i_l^{\mathrm{d}}, i_l^{\mathrm{q}}, i_o^{\mathrm{d}}, i_o^{\mathrm{q}}, v_o^{\mathrm{d}}, v_o^{\mathrm{q}}]^{\mathrm{T}}$, $x_{\mathrm{CC}} = [\gamma^{\mathrm{d}}, \gamma^{\mathrm{q}}]^{\mathrm{T}}$, $x_{\mathrm{PC}} = [p_{\mathrm{avg}}, q_{\mathrm{avg}}, \phi_p, \phi_q]^{\mathrm{T}}$, and $x_{\mathrm{PLL}} = [v_{\mathrm{PLL}}, \phi_{\mathrm{PPL}}, \delta]^{\mathrm{T}}$. Then, we can write (3) as

$$\begin{bmatrix} \dot{x}_{LCL} \\ \dot{x}_{\mathrm{CC}} \\ \dot{x}_{\mathrm{PC}} \\ \dot{x}_{\mathrm{PLL}} \end{bmatrix} = \begin{bmatrix} A_{LCL} & A_{LCL}^{\mathrm{CC}} & A_{LCL}^{\mathrm{PC}} & 0_{6\times 3} \\ A_{\mathrm{CC}}^{LCL} & 0_{2\times 2} & A_{\mathrm{CC}}^{\mathrm{PC}} & 0_{2\times 3} \\ 0_{4\times 6} & 0_{4\times 2} & A_{\mathrm{PC}} & 0_{4\times 3} \\ 0_{4\times 6} & 0_{4\times 2} & 0_{4\times 4} & A_{\mathrm{PLL}} \end{bmatrix}\begin{bmatrix} x_{LCL} \\ x_{\mathrm{CC}} \\ x_{\mathrm{PC}} \\ x_{\mathrm{PLL}} \end{bmatrix} + \begin{bmatrix} B_{LCL} \\ B_{\mathrm{CC}} \\ B_{\mathrm{PC}} \\ 0_{3\times 2} \end{bmatrix} u_1 + g(x, u_2),$$

where the nonzero submatrices A_{LCL}, A_{LCL}^{CC}, A_{LCL}^{PC}, A_{CC}^{LCL},

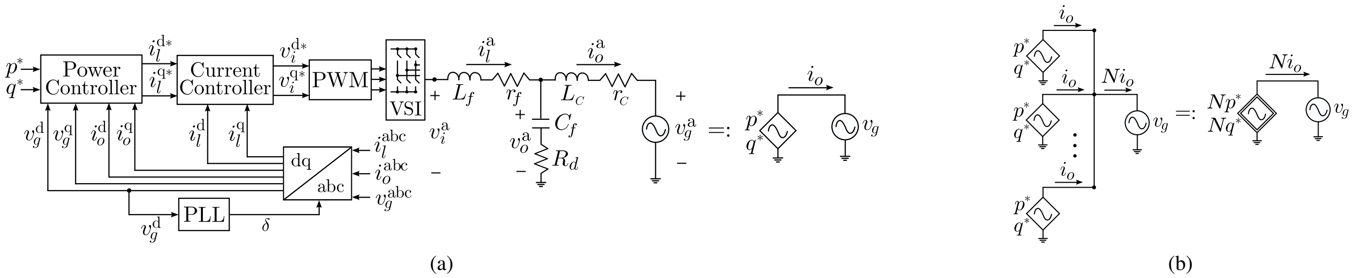

Fig. 1: (a) Block diagram of the grid-tied three phase inverter (one phase of the LCL filter and grid is depicted) and adopted shorthand. (b) Parallel connection of N identical inverters and the adopted shorthand representation of the reduced-order model.

$A_{\mathrm{CC}}^{\mathrm{PC}}$, A_{PC}, A_{PLL}, B_{LCL}, B_{CC}, and B_{PC} are given by

$$A_{LCL} = \begin{bmatrix} -\frac{k_{i\mathrm{d}}^p + r_f}{L_f} & 0 & 0 & 0 & -\frac{1}{L_f} & 0 \\ 0 & -\frac{k_{i\mathrm{d}}^p + r_f}{L_f} & 0 & 0 & 0 & -\frac{1}{L_f} \\ 0 & 0 & -\frac{r_c}{L_c} & \omega_{\mathrm{n}} & \frac{1}{L_c} & 0 \\ 0 & 0 & \omega_{\mathrm{n}} & -\frac{r_c}{L_c} & 0 & \frac{1}{L_c} \\ \frac{-R_d(k_{i\mathrm{d}}^p + r_f)}{L_f} + \frac{1}{C_f} & -\omega_{\mathrm{n}} R_d & \frac{R_d r_c}{L_c} - \frac{1}{C_f} & 0 & -R_d(\frac{1}{L_c} + \frac{1}{L_f}) & \omega_{\mathrm{n}} \\ \omega_{\mathrm{n}} R_d & \frac{-R_d(k_{i\mathrm{d}}^p + r_f)}{L_f} + \frac{1}{C_f} & 0 & R_d \frac{r_c}{L_c} - \frac{1}{C_f} & -\omega_{\mathrm{n}} & -R_d(\frac{1}{L_c} + \frac{1}{L_f}) \end{bmatrix},$$

$$A_{LCL}^{\mathrm{CC}} = \begin{bmatrix} \frac{k_{i\mathrm{d}}^i}{L_f} & 0 \\ 0 & \frac{k_{i\mathrm{q}}^i}{L_f} \end{bmatrix},\ A_{\mathrm{CC}}^{LCL} = \begin{bmatrix} -1 & 0 & 0 & 0 & 0 & 0 \\ 0 & -1 & 0 & 0 & 0 & 0 \end{bmatrix},$$

$$A_{LCL}^{\mathrm{PC}} = \begin{bmatrix} 0 & -\frac{k_{i\mathrm{d}}^p}{L_f} k_Q^p & 0 & \frac{k_{i\mathrm{d}}^p}{L_f} k_Q^i \\ -\frac{k_{i\mathrm{q}}^p}{L_f} k_P^p & 0 & \frac{k_{i\mathrm{q}}^p}{L_f} k_P^i & 0 \end{bmatrix},$$

$$A_{\mathrm{CC}}^{\mathrm{PC}} = \begin{bmatrix} 0 & -k_Q^p & 0 & k_Q^i \\ -k_P^p & 0 & k_P^i \end{bmatrix},$$

$$A_{\mathrm{PC}} = \begin{bmatrix} -\omega_c & 0 & 0 & 0 \\ 0 & -\omega_c & 0 & 0 \\ -1 & 0 & 0 & 0 \\ 0 & -1 & 0 & 0 \end{bmatrix},$$

$$A_{\mathrm{PLL}} = \begin{bmatrix} -\omega_{c,\mathrm{PLL}} & 0 & 0 \\ -1 & 0 & 0 \\ -k_{\mathrm{PLL}}^p & k_{\mathrm{PLL}}^i & 0 \end{bmatrix},$$

$$B_{LCL} = \begin{bmatrix} 0 & \frac{k_{i\mathrm{d}}^p}{L_f} k_Q^p \\ \frac{k_{i\mathrm{q}}^p}{L_f} k_P^p & 0 \\ 0 & 0 \\ 0 & 0 \\ 0 & \frac{k_{i\mathrm{d}}^p}{L_f} k_Q^p R_d \\ \frac{k_{i\mathrm{q}}^p}{L_f} k_P^p R_d & 0 \end{bmatrix},\ B_{\mathrm{CC}} = \begin{bmatrix} 0 & k_Q^p \\ k_P^p & 0 \end{bmatrix},$$

$$B_{\mathrm{PC}} = \begin{bmatrix} 0 & 0 \\ 0 & 0 \\ 1 & 0 \\ 0 & 1 \end{bmatrix}.$$

where $\omega_{\mathrm{n}} := 2\pi \times 60$. The nonzero entries of $g(x, u_2)$ are given by

$$\begin{aligned} g_3(x,u_2) &= (-k_{\mathrm{PLL}}^p v_{\mathrm{PLL}} + k_{\mathrm{PLL}}^i \phi_{\mathrm{PLL}}) i_o^{\mathrm{q}} - \frac{1}{L_c} v_g^{\mathrm{d}}(x,u_2), \\ g_4(x,u_2) &= (k_{\mathrm{PLL}}^p v_{\mathrm{PLL}} - k_{\mathrm{PLL}}^i \phi_{\mathrm{PLL}}) i_o^{\mathrm{d}} - \frac{1}{L_c} v_g^{\mathrm{q}}(x,u_2), \\ g_5(x,u_2) &= (-k_{\mathrm{PLL}}^p v_{\mathrm{PLL}} + k_{\mathrm{PLL}}^i \phi_{\mathrm{PLL}})(-R_d i_l^{\mathrm{q}} + v_o^{\mathrm{q}}) \\ &\quad + \frac{R_d}{L_c} v_g^{\mathrm{d}}(x,u_2), \\ g_6(x,u_2) &= (k_{\mathrm{PLL}}^p v_{\mathrm{PLL}} - k_{\mathrm{PLL}}^i \phi_{\mathrm{PLL}})(-R_d i_l^{\mathrm{d}} + v_o^{\mathrm{d}}) \\ &\quad + \frac{R_d}{L_c} v_g^{\mathrm{q}}(x,u_2), \\ g_9(x,u_2) &= \frac{3}{2}\omega_c \left(v_g^{\mathrm{d}}(x,u_2) i_o^{\mathrm{d}} + v_g^{\mathrm{q}}(x,u_2) i_o^{\mathrm{q}} \right), \\ g_{10}(x,u_2) &= \frac{3}{2}\omega_c \left(v_g^{\mathrm{q}}(x,u_2) i_o^{\mathrm{d}} - v_g^{\mathrm{d}}(x,u_2) i_o^{\mathrm{q}} \right), \\ g_{13}(x,u_2) &= \omega_{c,\mathrm{PLL}} v_g^{\mathrm{d}}(x,u_2), \\ g_{15}(x,u_2) &= \omega_{\mathrm{n}}, \end{aligned}$$

with $v_g^{\mathrm{d}}(x,u_2)$ and $v_g^{\mathrm{q}}(x,u_2)$ given by

$$\begin{aligned} v_g^{\mathrm{d}}(x,u_2) &= \frac{2}{3}\Big(\cos(\delta) v_g^{\mathrm{a}} + \cos(\delta - \frac{2\pi}{3}) v_g^{\mathrm{b}} \\ &\quad + \cos(\delta + \frac{2\pi}{3}) v_g^{\mathrm{c}} \Big), \\ v_g^{\mathrm{q}}(x,u_2) &= \frac{2}{3}\Big(\sin(\delta) v_g^{\mathrm{a}} + \sin(\delta - \frac{2\pi}{3}) v_g^{\mathrm{b}} \\ &\quad + \sin(\delta + \frac{2\pi}{3}) v_g^{\mathrm{c}} \Big). \end{aligned}$$

B. Reduced-order Model of Parallel-connected Inverters

Consider a collection of N identical inverters connected in parallel to the grid bus (see Fig. 1b). We have shown in [5] that this system of inverters can be represented by a single inverter with the same structure and model order as any individual inverter in the system, and that the aggregated inverter model exactly captures the input-output behaviour of the multi-inverter system. This is summarized next.

Replace the individual inverter model parameters $L_f, r_f, C_f, R_d, L_c, r_c, k_{\mathrm{id}}^p, k_{\mathrm{iq}}^p, k_{\mathrm{id}}^i, k_{\mathrm{id}}^i$ with $N^{-1}L_f, N^{-1}r_f, NC_f, N^{-1}R_d, N^{-1}L_c, N^{-1}r_c, N^{-1}k_{\mathrm{id}}^p$, $N^{-1}k_{\mathrm{iq}}^p, N^{-1}k_{\mathrm{id}}^i, N^{-1}k_{\mathrm{iq}}^i$. Then, we obtain the reduced-order model for the parallel system

$$\dot{x}^{\mathrm{r}} = A^{\mathrm{r}}x^{\mathrm{r}} + B^{\mathrm{r}}u_1^{\mathrm{r}} + g^{\mathrm{r}}(x^{\mathrm{r}}, u_2^{\mathrm{r}}), \tag{4}$$

where the inputs are $u_1^{\mathrm{r}} = Nu_1$ and $u_2^{\mathrm{r}} = u_2 = v_g^{\mathrm{abc}}$. Notice that the matrices $A^{\mathrm{r}} \in \mathbb{R}^{15\times15}$, $B^{\mathrm{r}} \in \mathbb{R}^{15\times2}$, and function $g^{\mathrm{r}} : \mathbb{R}^{15} \times \mathbb{R}^3 \to \mathbb{R}^{15}$ have the same structure as A, B, and g for the individual model. Next, we establish the connection between the dynamics of the individual and the reduced-order inverters. To aid this derivation, define vector $\eta := [N1_4^{\mathrm{T}}, 1_2^{\mathrm{T}}, N1_6^{\mathrm{T}}, 1_3^{\mathrm{T}}]^{\mathrm{T}}$.

Proposition 1. Consider the dynamics of the individual inverter and reduced-order aggregate model in (3) and (4), respectively. Suppose the initial conditions for the two dynamical systems at some time $t_0 \geq 0$ are such that $x^{\mathrm{r}}(t_0) = \mathrm{diag}(\eta)x(t_0)$. If $u_1^{\mathrm{r}} = Nu_1$ and $u_2^{\mathrm{r}} = u_2$, it follows that $x^{\mathrm{r}}(t) = \mathrm{diag}(\eta)x(t),\ \forall t \geq t_0$.

Proof. Permute the state vector as $\widehat{x} := [i_l^{\mathrm{d}}, i_l^{\mathrm{q}}, i_o^{\mathrm{d}}, i_o^{\mathrm{q}}, \gamma^{\mathrm{d}}, \gamma^{\mathrm{q}}, p_{\mathrm{avg}}, q_{\mathrm{avg}}, \phi_p, \phi_q, v_o^{\mathrm{d}}, v_o^{\mathrm{q}}, v_{\mathrm{PLL}}, \phi_{\mathrm{PPL}}, \delta]^{\mathrm{T}}$, and subsequently η as $\widehat{\eta} := [N1_{10}^{\mathrm{T}}, 1_5^{\mathrm{T}}]^{\mathrm{T}}$. The result can then be proved following [5], with the so-called power-scaling parameter picked as $\underline{\kappa} = \widehat{\eta}$. □

In this result, the scaling of the reference active- and reactive-power setpoints by the number of inverters signifies the collective input of the parallel system. Notice that all the currents in the model and the controller states (except those of the PLL) are scaled while the voltages and PLL states remain the same as the individual inverters. The following establishes that the output of the reduced-order model is the same as the collective output of the multi-inverter system.

Remark. The output current of the reduced-order model is given by

$$i_o^{\mathrm{dr}}(t) = Ni_o^{\mathrm{d}}(t), \quad i_o^{\mathrm{qr}}(t) = Ni_o^{\mathrm{q}}(t). \tag{5}$$

With the aggregation of the parallel system established above, we bring attention to Fig. 2b that illustrates the main goal and contribution of this paper. We consider a collection of N identical inverters connected to an arbitrary network represented by the admitance matrix Y. In order to leverage the parallel aggregation in this setup, we create an auxiliary bus, and we transfer all the inverters to this bus. Then, we aggregate the inverters into a single inverter using the parallel aggregation approach outlined above. Following this, the injections to the grid can be expressed as a linear function of the output current of the aggregated inverter model.

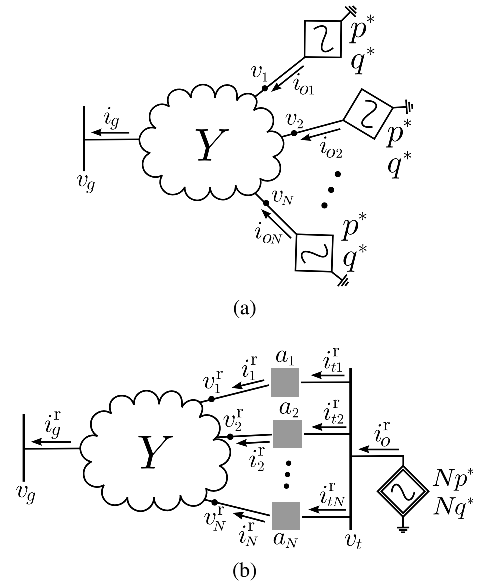

Fig. 2: (a) Network of N identical inverters (b) Reduced-order model of the system of inverters.

III. Aggregation of Inverters in Networks with Arbitrary Topologies

In this section, we extend the model reduction method for parallel inverters to networks with arbitrary topologies. We begin this section by describing the model of the network. Then, we outline the aggregation approach and present an approach that leverages a linearization of the AC power-flow equations to facilitate the derivation of the reduced-order model.

A. Network Description

We consider an electrical network with admittance matrix Y, composed of N identical inverters and a grid bus (see Fig. 2a; each inverter is pictorially represented with the shorthand established in Fig. 1a). Suppose the nodes of the electrical network and the grid are collected in the set $\mathcal{A}$, and the branches are collected in the set $\mathcal{E} := \{(k,\ell) \subset \mathcal{A} \times \mathcal{A}\}$. Let $i_{\mathcal{A}} \in \mathbb{C}^{|\mathcal{A}|}$ and $v_{\mathcal{A}} \in \mathbb{C}^{|\mathcal{A}|}$ denote the vectors that collect the nodal current injections and node voltages in the network (including grid bus), respectively. It follows from Kirchhoff's and Ohm's laws that

$$i_{\mathcal{A}} = Yv_{\mathcal{A}}, \tag{6}$$

where the entries of the admittance matrix $Y \in \mathbb{C}^{|\mathcal{A}|\times|\mathcal{A}|}$ are given by

$$[Y]_{k\ell} := \begin{cases} y_k + \sum_{(k,d)\in\mathcal{E}} y_{kd}, & \text{if } k = \ell, \\ -y_{k\ell}, & \text{if } (k,\ell) \in \mathcal{E}, \\ 0, & \text{otherwise}, \end{cases}$$

with y_k denoting the shunt admittance at node k, and $y_{k\ell}$ the admittance of the line (k,ℓ). Let $\mathcal{I}$ denote the index set of inverter buses, $\mathcal{N} := \mathcal{I} \bigcup \{g\}$ denote the index set of the grid and inverter buses, and $\mathcal{Z} := \mathcal{A} \setminus \mathcal{N}$ the index set of zero injection buses. Then, we can rewrite (6) as

$$\begin{bmatrix} i_{\mathcal{N}} \\ 0_{|\mathcal{Z}|} \end{bmatrix} = \begin{bmatrix} Y_{\mathcal{N}\mathcal{N}} & Y_{\mathcal{N}\mathcal{Z}} \\ Y_{\mathcal{N}\mathcal{Z}}^{\mathrm{T}} & Y_{\mathcal{Z}\mathcal{Z}} \end{bmatrix} \begin{bmatrix} v_{\mathcal{N}} \\ v_{\mathcal{Z}} \end{bmatrix}. \tag{7}$$

Then, we obtain the following relationship between the current injections and terminal voltages for buses with non-zero injections:

$$i_{\mathcal{N}} = \left(Y_{\mathcal{N}\mathcal{N}} - Y_{\mathcal{N}\mathcal{Z}} Y_{\mathcal{Z}\mathcal{Z}}^{-1} Y_{\mathcal{N}\mathcal{Z}}^{\mathrm{T}}\right) v_{\mathcal{N}} =: Y_{\mathrm{red}}\, v_{\mathcal{N}}, \quad (8)$$

where, invertibility of the submatrix $Y_{\mathcal{Z}\mathcal{Z}}$ follows from the connectivity of the network [23]. For subsequent developments, we find it useful to partition Y_{red} as follows:

$$\begin{bmatrix} -i_g \\ i_{\mathcal{I}} \end{bmatrix} = \begin{bmatrix} Y_{gg} & Y_{g\mathcal{I}} \\ Y_{g\mathcal{I}}^{\mathrm{T}} & Y_{\mathcal{I}\mathcal{I}} \end{bmatrix} \begin{bmatrix} v_g \\ v_{\mathcal{I}} \end{bmatrix}. \quad (9)$$

Note that the negative sign that precedes i_g is in acknowledgment of its assumed direction as shown in Fig. 2a.

B. Model Reduction Procedure

With the distribution-network model in place, we now describe the model-reduction procedure to aggregate the N inverters. The procedure involves introducing an auxiliary bus with the aid of appropriately defined (fictitious) transformers (see Fig. 2b) and *transferring* all inverters to this bus. We define the transformer side that is connected to the auxiliary bus as primary, and the side connected to the electrical network as secondary. With all N inverters at the auxiliary bus, we can use the method outlined in Section II-B to obtain a reduced-order model. Indeed, the key design choice in this process is the auxiliary-bus voltage. While there are an infinite number of choices for this, we adopt the average of the inverter terminal voltages in the original network, and determine these voltages with a linearization of the power-flow equations. The steps outlined above are detailed next:

1) Network equations with auxiliary bus: Let $v_{t\mathrm{DQ}} := v_t^{\mathrm{D}} + j v_t^{\mathrm{Q}} \in \mathbb{C}$ denote the pre-determined voltage of the auxiliary bus in the DQ-frame, and $a_{\mathrm{DQ}} \in \mathbb{C}^N$ denote the vector that collects the complex-valued turns ratios of the transformers. As discussed above, we choose $v_{t\mathrm{DQ}}$ to be the average of entries in $v_{\mathcal{I}\mathrm{DQ}}$, that is:

$$v_{t\mathrm{DQ}} = \frac{1}{N} 1_N^{\mathrm{T}} v_{\mathcal{I}\mathrm{DQ}}. \quad (10)$$

With the inverters transferred to this auxiliary bus, we obtain the reduced-order model following the method outlined in Section II-B and sketched in Fig. 2b. Let $i_{o\mathrm{DQ}}^{\mathrm{r}} \in \mathbb{C}$ denote the output current of the aggregated inverter in the DQ-frame, $i_{t\mathrm{DQ}} \in \mathbb{C}^N$ captures the currents from the auxiliary bus into the primary side of the transformers, $i_{\mathcal{I}\mathrm{DQ}}^{\mathrm{r}} \in \mathbb{C}^N$ captures the currents from the secondary-side of the transformers into the electrical network, and $i_{g\mathrm{DQ}}^{\mathrm{r}} \in \mathbb{C}$ denotes the grid current injection in the DQ-frame (see Fig. 2b). Elementarily, we recognize that

$$i_{o\mathrm{DQ}}^{\mathrm{r}} = 1_N^{\mathrm{T}} i_{t\mathrm{DQ}}. \quad (11)$$

Furthermore, we also have

$$v_{\mathcal{I}\mathrm{DQ}}^{\mathrm{r}} = a_{\mathrm{DQ}} v_{t\mathrm{DQ}}, \quad i_{\mathcal{I}\mathrm{DQ}}^{\mathrm{r}} = \mathrm{diag}(a_{\mathrm{DQ}}^{\mathrm{H}})^{-1} i_{t\mathrm{DQ}}, \quad (12)$$

where $v_{\mathcal{I}\mathrm{DQ}}^{\mathrm{r}}$ is the vector of transformer secondary-side voltages (see Fig. 2b). From (9), we can write:

$$i_{g\mathrm{DQ}}^{\mathrm{r}} = -Y_{gg} v_{g\mathrm{DQ}} - Y_{g\mathcal{I}} a_{\mathrm{DQ}} v_{t\mathrm{DQ}}, \quad (13)$$

$$\mathrm{diag}(a_{\mathrm{DQ}}^{\mathrm{H}})^{-1} i_{t\mathrm{DQ}}^{\mathrm{r}} = Y_{g\mathcal{I}}^{\mathrm{T}} v_{g\mathrm{DQ}} + Y_{\mathcal{I}\mathcal{I}} a_{\mathrm{DQ}} v_{t\mathrm{DQ}}, \quad (14)$$

where we have substituted for $v_{\mathcal{I}\mathrm{DQ}}^{\mathrm{r}}$ and $i_{\mathcal{I}\mathrm{DQ}}^{\mathrm{r}}$ from (12). Eliminating $v_{t\mathrm{DQ}}$ from (13) and (14) and using (11) yields the following expression for the current injected into the grid as a function of the output current of the aggregate inverter model:

$$i_{g\mathrm{DQ}}^{\mathrm{r}} = -Y_{gg} v_{g\mathrm{DQ}} - Y_{g\mathcal{I}} a_{\mathrm{DQ}} \left(\frac{i_{o\mathrm{DQ}}^{\mathrm{r}} - a_{\mathrm{DQ}}^{\mathrm{H}} Y_{g\mathcal{I}}^{\mathrm{T}} v_{g\mathrm{DQ}}}{a_{\mathrm{DQ}}^{\mathrm{H}} Y_{\mathcal{I}\mathcal{I}} a_{\mathrm{DQ}}} \right). \quad (15)$$

With this in place, the active and reactive power injection to the grid bus, denoted by p_g^{r} and q_g^{r}, respectively, are given by

$$p_g^{\mathrm{r}} = \frac{3}{2}(v_g^{\mathrm{D}} i_g^{\mathrm{Dr}} + v_g^{\mathrm{Q}} i_g^{\mathrm{Qr}}), \quad (16)$$

$$q_g^{\mathrm{r}} = \frac{3}{2}(v_g^{\mathrm{Q}} i_g^{\mathrm{Dr}} - v_g^{\mathrm{D}} i_g^{\mathrm{Qr}}). \quad (17)$$

2) Linear approximation to AC power-flow to obtain auxiliary-bus voltage: Next, we bring attention to the turns ratio and pre-determined auxiliary-bus voltage calculation in (12) and (10), respectively. Notice that the calculations require the actual terminal voltages of the inverter buses, i.e., the vector $v_{\mathcal{I}\mathrm{DQ}}$. These voltages can be obtained from the solution of the nonlinear algebraic power-flow equations for the network; however, this presents significant computational burden and would render the reduced-order model to also be a differential-algebraic-equation model. To circumvent this, we resort to a linear approximation of the AC power-flow equations to obtain the power flow solutions. The pertinent steps involved in this approach are summarized next:

1) The inverter parameters, reference-power setpoints, and the grid voltage are converted into per unit (p.u.), with $|v_g|$ serving as the voltage base.
2) We pick the linearization point to be the no-load voltage—this is the voltage profile in the network with zero power injections at the inverter buses—as in [11]. This is denoted by $v_{\mathcal{I}}^{\star} \in \mathbb{C}^N$, and it follows from (9) that it is given by

$$v_{\mathcal{I}}^{\star} = -Y_{\mathcal{I}\mathcal{I}}^{-1} Y_{g\mathcal{I}}^{\mathrm{T}} v_g. \quad (18)$$

Then, the linear approximation to $v_{\mathcal{I}}$ in rectangular coordinates is given by [11]

$$\begin{aligned} \mathrm{Re}\{v_{\mathcal{I}}\} &= \mathrm{Re}\{v_{\mathcal{I}}^{\star}\} + \Gamma p_{\phi}^{*} + \Lambda q_{\phi}^{*}, \\ \mathrm{Im}\{v_{\mathcal{I}}\} &= \mathrm{Im}\{v_{\mathcal{I}}^{\star}\} + \Lambda p_{\phi}^{*} - \Gamma q_{\phi}^{*}, \end{aligned} \quad (19)$$

where $p_{\phi}^{*} := \frac{1}{3} 1_N p^{*}$ and $q_{\phi}^{*} := \frac{1}{3} 1_N q^{*}$ are the inverter bus active and reactive power injections in a per-phase equivalent sense, respectively, and the matrices Γ and Λ are given by

$$\begin{aligned} \Gamma &:= R\mathrm{diag}\left(\frac{\cos \angle v_{\mathcal{I}}^{\star}}{|v_{\mathcal{I}}^{\star}|}\right) - X\mathrm{diag}\left(\frac{\sin \angle v_{\mathcal{I}}^{\star}}{|v_{\mathcal{I}}^{\star}|}\right), \\ \Lambda &:= X\mathrm{diag}\left(\frac{\cos \angle v_{\mathcal{I}}^{\star}}{|v_{\mathcal{I}}^{\star}|}\right) + R\mathrm{diag}\left(\frac{\sin \angle v_{\mathcal{I}}^{\star}}{|v_{\mathcal{I}}^{\star}|}\right), \end{aligned} \quad (20)$$

TABLE I: Inverter Parameters

LCL filter		Current Controller		PLL	
L_f	1.0 mH	k_{id}^{p}, k_{iq}^{p}	6	k_{PLL}^{p}	1.25
r_f	0.7 Ω	k_{id}^{i}, k_{iq}^{i}	350	k_{PLL}^{i}	10
C_f	24 mF			$\omega_{c,\text{PLL}}$	$2\pi \times 200$
R_d	0.02 Ω	Power Controller			
L_c	0.2 mH	k_{P}^{p}, k_{Q}^{p}	0.01		
r_c	0.12 Ω	k_{P}^{i}, k_{Q}^{i}	0.1		
		ω_c	50.26		

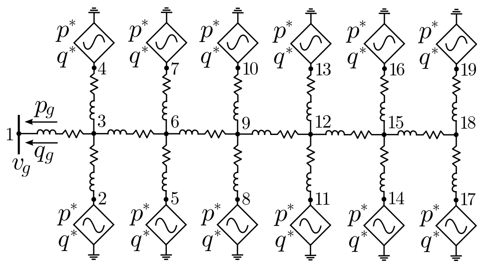

(a)

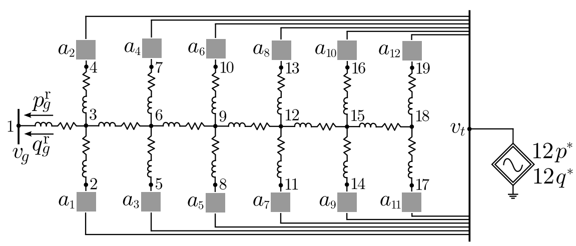

(b)

Fig. 3: (a) Test network considered in the case studies is composed of 19 buses and 12 identical inverters. With regard to the notation established in Section III-A, it follows that $\mathcal{A} = \{1, \ldots, 19\}$, $\mathcal{I} = \{2, 4, 5, 7, 8, 10, 11, 13, 14, 16, 17, 19\}$, and $\mathcal{Z} = \{3, 6, 9, 12, 15, 18\}$. (b) Reduced-order model of the 19-bus system.

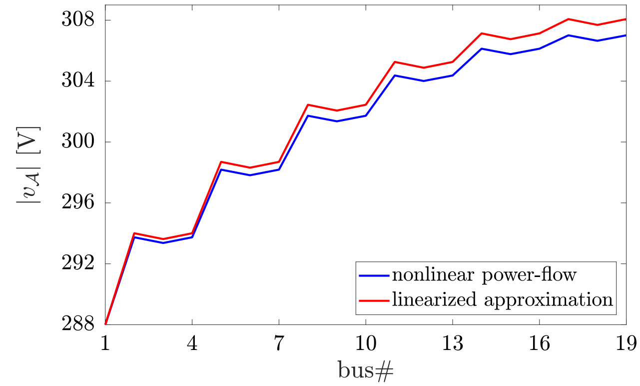

(a) Voltage magnitude

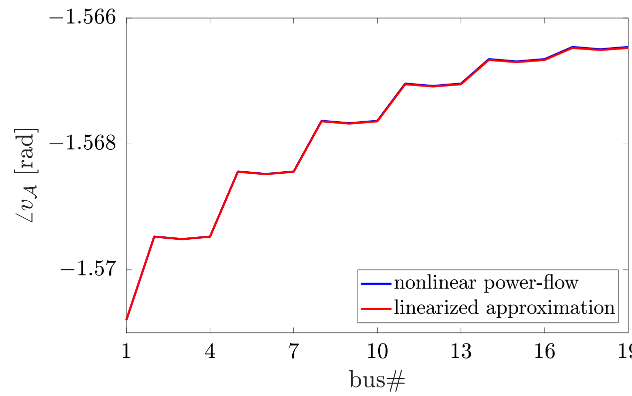

(b) Voltage angle

Fig. 4: Accuracy of the linear approximation for the test case.

where $R := \text{Re}\{Y_{\mathcal{I}\mathcal{I}}^{-1}\}$ and $X := \text{Im}\{Y_{\mathcal{I}\mathcal{I}}^{-1}\}$.

3) Using (1) with transformation matrix $\Psi(\delta_g)$, we obtain solutions in the global DQ frame.

IV. Simulation Results

In this section, we validate the model-reduction method with numerical simulation results for a system of 12 inverters connected in the network described in [24]. The original network is sketched in Fig. 3a, and the network with the aggregated inverter is shown in Fig. 3b. The voltage and frequency of the grid are 288V and $2\pi \times 60$ rad/s, respectively. The filter and controller parameters of each inverter are listed in Table I. The simulation is performed on a personal computer with a Intel Core i7-7700HQ processor @ 2.80GHz CPU and 8GB RAM.

First, we establish the accuracy of the linear approximation. To this end, the comparison of the nonlinear AC power-flow solution obtained using Matpower [25] and the linear approximation when $p^* = 3$kW and $q^* = 0$VAR is shown in Fig. 4. Next, we validate the accuracy of the reduced-order model with time-domain simulations. The following simulations are performed: 1) Step change in p^* from 3kW to 3.2kW at $t = 1$s, and 3.2kW to 3kW at $t = 1.03$s. 2) Step change in q^* from 0VAR to 100VAR at $t = 1$s, and 100VAR to 0VAR at $t = 1.03$s. For both cases, we stop the simulation at $t = 1.06$s. The running time of the original system for case #1 and #2 are 2.35s and 2.31s, respectively, and of the reduced-order model are 0.92s and 0.90s, respectively. Computation times indicate the usefulness of the proposed model-reduction method. To validate the accuracy of the model-reduction method, we compare the injected active and reactive power to the grid bus in Fig. 5 and Fig. 6 for case #1 and #2, respectively. We also plot results for the case when the network is ignored, and all inverters are connected in parallel to the grid bus (see Fig. 1b, with $N = 12$). The figures show that the parallel approximation yields significant error in the grid injection since power losses in the system are being neglected, and all inverters sense a common terminal voltage.

V. Concluding Remarks and Directions for Future Work

In this paper, we outlined a model-reduction method to develop an aggregate model for a collection of inverters connected in an arbitrary electrical network. The foundations

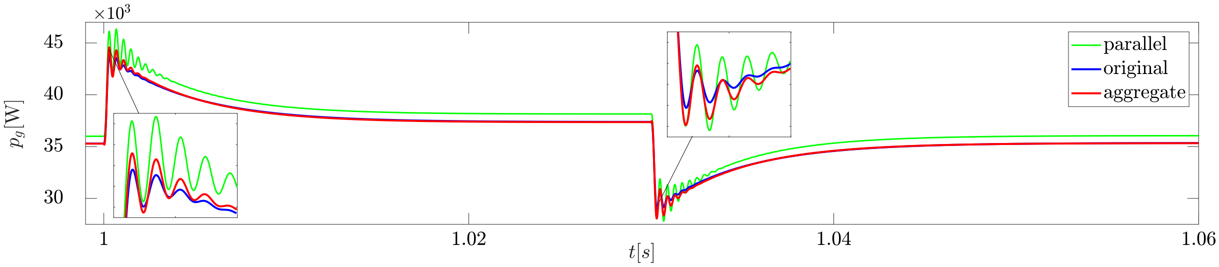

(a) Active power injection to the grid bus

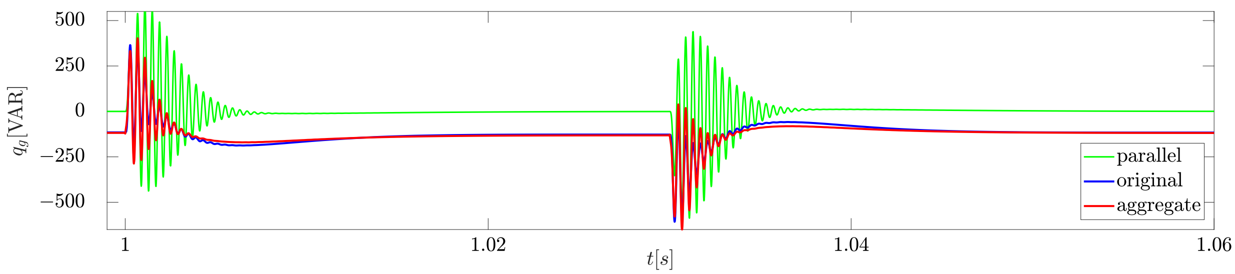

(b) Reactive power injection to the grid bus

Fig. 5: Simulation results for case #1: Active power setpoint p^* is 3kW for $t < 1$s, 3.2kW for $1 \leq t < 1.03$s, and 3kW for $t \geq 1.03$s.

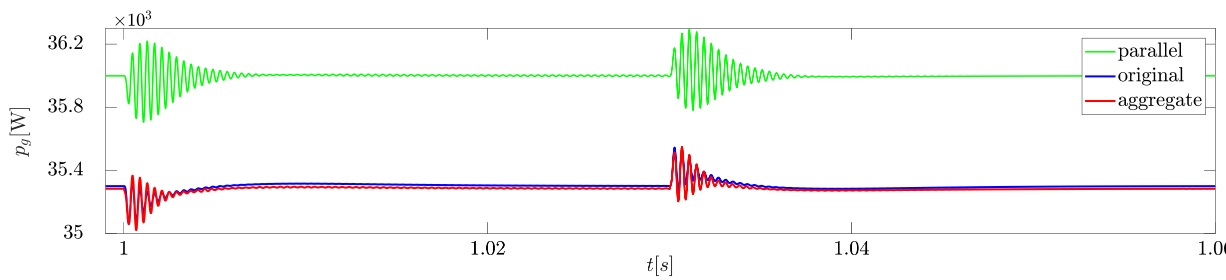

(a) Active power injection to the grid bus

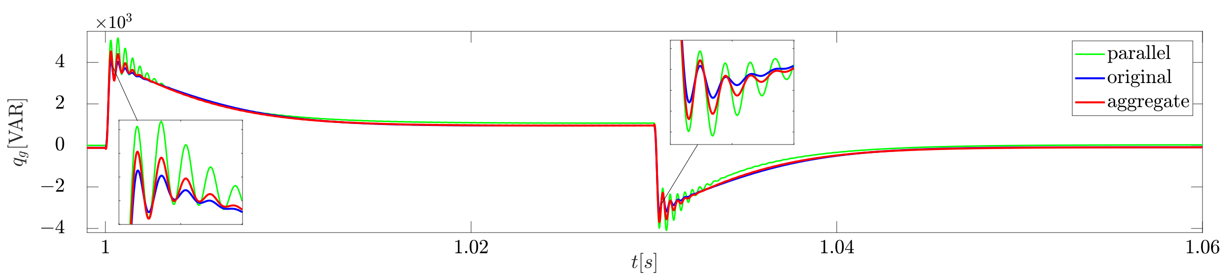

(b) Reactive power injection to the grid bus

Fig. 6: Simulation results for case #2: Reactive power setpoint q^* is 0VAR for $t < 1$s, 100VAR for $1 \leq t < 1.03$s, and 0VAR for $t \geq 1.03$s.

of this method were: i) our previous work on the derivation of a lumped-parameter reduced-order aggregate model for parallel-connected grid-tied three-phase inverters, and ii) classical results on aggregation of coherent synchronous generators. Precisely, the approach we outline involves transferring all inverters to an auxiliary bus with the aid of ideal transformers and suitable linearizations of the AC power-flow equations. We showed that the numerical simulations of the aggregated model were fairly accurate when compared to the original system. As part of future work, we plan to further improve transient performance by clustering inverters systematically into multiple groups.

References

[1] M. Rasheduzzaman, J. A. Mueller, and J. W. Kimball, "An accurate small-signal model of inverter- dominated islanded microgrids using *dq* reference frame," *IEEE Journal of Emerging and Selected Topics in Power Electronics*, vol. 2, pp. 1070–1080, Dec 2014.

[2] J. A. Mueller, M. Rasheduzzaman, and J. W. Kimball, “A model modification process for grid-connected inverters used in islanded microgrids,” *IEEE Transactions on Energy Conversion*, vol. 31, pp. 240–250, March 2016.

[3] M. Prodanovic and T. C. Green, “Control and filter design of three-phase inverters for high power quality grid connection,” *IEEE Transactions on Power Electronics*, vol. 18, pp. 373–380, Jan 2003.

[4] E. Twining and D. G. Holmes, “Grid current regulation of a three-phase voltage source inverter with an lcl input filter,” *IEEE Transactions on Power Electronics*, vol. 18, pp. 888–895, May 2003.

[5] V. Purba, S. V. Dhople, S. Jafarpour, F. Bullo, and B. B. Johnson, “Reduced-order structure-preserving model for parallel-connected three-phase grid-tied inverters,” in *2017 IEEE 18th Workshop on Control and Modeling for Power Electronics (COMPEL)*, pp. 1–7, July 2017.

[6] A. J. Germond and R. Podmore, “Dynamic aggregation of generating unit models,” *IEEE Transactions on Power Apparatus and Systems*, vol. PAS-97, pp. 1060–1069, July 1978.

[7] M. L. Ourari, L. A. Dessaint, and V.-Q. Do, “Dynamic equivalent modeling of large power systems using structure preservation technique,” *IEEE Transactions on Power Systems*, vol. 21, pp. 1284–1295, Aug 2006.

[8] J. H. Chow, *Power System Coherency and Model Reduction*. Springer, 2013.

[9] A. Ishchenko, J. M. A. Myrzik, and W. L. Kling, “Dynamic equivalencing of distribution networks with dispersed generation using hankel norm approximation,” *IET Generation, Transmission Distribution*, vol. 1, pp. 818–825, Sept 2007.

[10] F. O. Resende, J. Matevosyan, and J. V. Milanovic, “Application of dynamic equivalence techniques to derive aggregated models of active distribution network cells and microgrids,” in *2013 IEEE Grenoble Conference*, pp. 1–6, June 2013.

[11] S. V. Dhople, S. S. Guggilam, and Y. C. Chen, “Linear approximations to ac power flow in rectangular coordinates,” in *2015 53rd Annual Allerton Conference on Communication, Control, and Computing (Allerton)*, pp. 211–217, Sept 2015.

[12] S. Bolognani and F. Dörfler, “Fast power system analysis via implicit linearization of the power flow manifold,” in *2015 53rd Annual Allerton Conference on Communication, Control, and Computing (Allerton)*, pp. 402–409, Sept 2015.

[13] S. Bolognani and S. Zampieri, “On the existence and linear approximation of the power flow solution in power distribution networks,” *IEEE Transactions on Power Systems*, vol. 31, pp. 163–172, Jan 2016.

[14] P. Kokotović, H. Khalil, and J. O’Reilly, *Singular Perturbation Methods in Control: Analysis and Design*. Society for Industrial and Applied Mathematics, 1999.

[15] L. Luo and S. V. Dhople, “Spatiotemporal model reduction of inverter-based islanded microgrids,” *IEEE Transactions on Energy Conversion*, vol. 29, pp. 823–832, December 2014.

[16] M. Rasheduzzaman, J. A. Mueller, and J. W. Kimball, “Reduced-order small-signal model of microgrid systems,” *IEEE Transactions on Sustainable Energy*, vol. 6, pp. 1292–1305, Oct 2015.

[17] O. O. Ajala, A. D. Domínguez-García, and P. W. Sauer, “A hierarchy of models for inverter-based microgrids,” in *Energy Markets and Responsive Grids: Modeling, Control and Optimization* (S. Meyn, T. Samad, S. Glavaski, I. Hiskens, and J. Stoustrup, eds.), Berlin: Springer-Verlag, 2017.

[18] P. J. Hart, R. H. Lasseter, and T. M. Jahns, “Reduced-order harmonic modeling and analysis of droop-controlled distributed generation networks,” in *IEEE 7th International Symposium on Power Electronics for Distributed Generation Systems (PEDG)*, pp. 1–9, June 2016.

[19] A. Ulbig, T. S. Borsche, and G. Andersson, “Impact of low rotational inertia on power system stability and operation,” 2014. [Online] Available at: `http://arxiv.org/abs/1312.6435`.

[20] T. S. Borsche, T. Liu, and D. J. Hill, “Effects of rotational inertia on power system damping and frequency transients,” in *2015 54th IEEE Conference on Decision and Control (CDC)*, pp. 5940–5946, Dec 2015.

[21] M. Pirani, J. W. Simpson-Porco, and B. Fidan, “System-theoretic performance metrics for low-inertia stability of power networks,” 2017. [Online] Available at: `http://arxiv.org/abs/1703.02646`.

[22] N. W. Miller, B. Leonardi, R. DAquila, and K. Clark, “Western wind and solar integration study phase 3a: low levels of synchronous generation,” tech. rep., NREL/TP-5D00-64822. Golden, Colorado: National Renewable Energy Laboratory, 2015.

[23] F. Dörfler and F. Bullo, “Kron reduction of graphs with applications to electrical networks,” *IEEE Transactions on Circuits and Systems I: Regular Papers*, vol. 60, pp. 150–163, January 2013.

[24] E. Dall’Anese, S. V. Dhople, and G. B. Giannakis, “Optimal dispatch of photovoltaic inverters in residential distribution systems,” *IEEE Transactions on Sustainable Energy*, vol. 5, pp. 487–497, April 2014.

[25] R. D. Zimmerman and C. E. Murillo-Sánchez, “Matpower 4.1 user’s manual,” 2011.